The Bell System Technical Journal
Vol. 55, No. 10, December 1976
Printed in U.S.A.

Wavelength Dependence of Frequency-Response Measurements In Multimode Optical Fibers

By L. G. COHEN, H. W. ASTLE, and I. P. KAMINOW

(Manuscript received May 24, 1976)

A newly developed technique for directly measuring fiber dispersion in the frequency domain as a function of wavelength is described. Spectrally filtered white light from a xenon arc lamp is sinusoidally modulated in the range 0 to 1 GHz by an electrooptic modulator and injected into a fiber. The procedure is to vary the modulation frequency and measure the corresponding sideband output power with a photomultiplier and spectrum analyzer. Ratio measurements between the test fiber and a short reference fiber give the baseband frequency response. A number of germanium- and boron-doped fibers have been examined. The least dispersive borosilicate graded-index fiber has a 1 dB bandwidth of 1 GHz, after 1.07 km of propagation at $\lambda = 908$ nm. The width broadens gradually with increasing wavelengths up to $\lambda = 1100$ nm.

I. INTRODUCTION

Optical fiber waveguides are potentially useful for transmitting analog signals as well as digital pulses in communication systems. The information-carrying capacity of such a waveguide is determined by its impulse response in the time domain or equivalently in the frequency domain by the spectral transfer function, which is the Fourier transform of the impulse response. Most of the previous studies[1] of fiber dispersion have analyzed the fiber response to short laser pulses. In these studies we are limited to wavelengths for which pulsed laser sources are available. The frequency domain method described here allows accurate measurements of fiber response to be made over a wide range of wavelengths using an incoherent broadband source, such as a xenon arc lamp.

The simplicity of the method rests on the observation[2] that for an incoherent optical carrier the fiber response behaves quasi-linearly in power. The implication for the optical power $p(t)$ and its transform

$P(\omega)$ is

$$P_{out}(\omega) = G(\omega) \times P_{in}(\omega) \tag{1}$$

or

$$p_{out}(t) = g(t) * p_{in}(t), \tag{2}$$

where $G(\omega)$ is the power transfer function of the baseband frequency ω, $g(t)$ is the power impulse response and $*$ denotes convolution. This quasi-linear behavior results when fluctuations in the optical carrier frequency are sufficiently large and rapid. Thus, the phase of an incoherent optical source of width $\Delta\lambda = 1$ nm fluctuates on average through one cycle in 3×10^{-12} s for $\lambda = 1000$ nm, but the characteristic time required to observe intensity modulation of the carrier at frequencies less than 10 GHz is greater than 10^{-10} seconds. Hence, the power-linearity approximation holds for most practical measurement methods utilizing sources whose spectral bandwidth ($\Delta\lambda$) is greater than 1 nm. Although (1) and (2) have been derived rigorously by Personick,[2] we present a simple physical derivation later in this paper.

Modern multimode fibers are fabricated with smoothly graded refractive index profiles that have a maximum on the core axis and decrease gradually with an approximately power law variation until they merge into the cladding region. The optimal profile, at a particular wavelength, is the one for which the group velocity variation from ray to ray most nearly compensates for the corresponding path length variation.[3] Dispersive refractive index differences between material constituents (B_2O_3 and SiO_2 for borosilicate fibers; GeO_2 and SiO_2 for germanium-doped fibers) causes modal group velocities to depend not only on the index profile but also on the wavelength (profile dispersion). Consequently, the exponential parameter, α, which characterizes the optimal profile, may deviate from $\alpha = 2$ and is wavelength dependent.[4–6] Recent experimental investigations have shown that graded-index fibers can reduce intermodal dispersion by almost two orders of magnitude from what it would be in a step ungraded-index multimode fiber.[7]

This paper describes a newly developed technique for directly measuring fiber baseband frequency response in spectrally filtered incoherent light. The spectral test set is particularly suitable for wavelength-dependent studies over a wide range of wavelengths without resorting to a multitude of monochromatic mode-locked laser sources. Instead of injecting pulses to measure a fiber's impulse response, we inject an incoherent cw optical carrier that is intensity-modulated by a frequency-tunable sinusoidal signal. Then, we compare the intensities of the sine wave envelopes at the input and output ends of the fiber. Sideband power is detected by a photomultiplier and displayed on a spectrum analyzer. The receiver dynamic range is sufficient to

measure transmission through kilometer-long fibers with an accuracy of ±10 percent over an electrical bandwidth of dc to 1 GHz and is equivalent to measuring $2\sigma \approx 0.1$ ns full rms impulse response widths. Measurement precision is better in the frequency domain than the time domain, because the deconvolution process, for removing signal distortion caused by the limited detector bandwidth, is simply an arithmetic division of output by input frequency response rather than a cumbersome deconvolution integral of pulse shapes. One shortcoming of the present technique is that we do not measure the input to output phase change of the sinusoidal modulation and therefore cannot construct the impulse response directly from the power frequency response data. However, approximate mathematical methods are available for determining the phase from the magnitude of a transfer function. Measurement of the phase change may also be feasible. Nevertheless, unless the phase distortion is extreme, the information capacity of the fiber will be indicated by the magnitude of the transfer function.

Previous dispersion measurements in the frequency domain were made by comparing the best spectra of longitudinal modes from a free-running laser before and after transmission through a fiber[8], by externally modulating a laser[9] or by directly modulating a light-emitting diode (LED).[10] One disadvantage of the technique described in Ref. 8 is that the fiber frequency response can only be measured at discrete frequencies corresponding to integral multiples of the longitudinal mode spacing of the laser (100-MHz increments for a 1.5-m cavity length). The other techniques were used to make frequency response measurements only at one wavelength from dc to several hundred MHz and had less dynamic range than our system. Personick et al. used wide bandwidth LED light ($\Delta\lambda \approx 40$ nm at $\lambda = 900$ nm) to measure primarily material dispersion effects in a 1-km fiber.[10] Our technique uses narrow spectral width incoherent light to measure primarily intermodal dispersion effects in kilometer-long fibers.

1.1 Technique and apparatus

The measuring apparatus is illustrated in Fig. 1. The xenon arc lamp output passes through one of a set of narrowband interference filters and is focused into a $LiTaO_3$ electrooptic intensity modulator. The modulated beam is then refocused into either the fiber under test or a short length (2 m) of reference fiber. The fiber output is then detected by a sensitive broadband photomultiplier and the baseband modulation components are displayed by a spectrum analyzer. The component at modulating frequency ω from the reference fiber is taken as $P_{in}(\omega)$ and the component from the test fiber as $P_{out}(\omega)$.

The $LiTaO_3$ modulator was designed[11] for use with a 1.06-μm laser

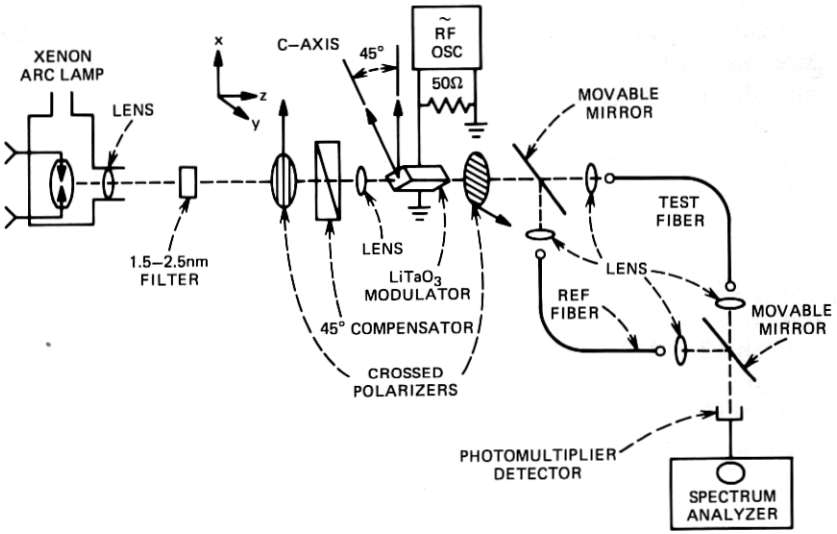

Fig. 1—Experimental arrangement for making spectral dispersion measurements in the frequency domain.

and has too small an aperture-to-length ratio to pass the focused incoherent beam completely. Nevertheless, it has proved adequate for these early measurements, while a more-suitable modulator was being built. The $LiTaO_3$ rod is 0.25 mm by 0.25 mm by 10 mm and its low-capacity coaxial housing allows for modulation frequencies above 1 GHz. Typically, 3 W of drive power from the rf sine wave generator is needed to provide 40-percent modulation. An Ehringhaus compensator biases the modulator in its linear region at the operating wavelength. The intensity transmitted by the $LiTaO_3$ crystal and compensator placed between crossed polarizers is proportional to $\sin^2 \Gamma/2$, where Γ is the phase retardation of crystal and compensator, consisting of a dc bias plus time-dependent term. Dispersion of the optical bias over the spectral width $\Delta\lambda$ of the input filter is an important consideration in system performance. For $LiTaO_3$ at $\lambda = 800$ nm,

$$d\Gamma_{dc}/d\lambda = \frac{2\pi L}{\lambda}\,(dB/d\lambda - B/\lambda) \approx -1.9 \times 10^{-2}\pi L, \qquad (3)$$

where Γ_{dc} is the phase retardation bias, λ is the wavelength in nm, L is the modulator length in mm, and B is the difference between extraordinary and ordinary refractive indices. For $L = 10$ mm and $\Delta\lambda = 1.5$ nm, the bias point is smeared by as much as 0.29π radians (neglecting the smaller effect of opposite sign due to the compensator). Thus, wavelengths at the spectral band edges will have somewhat

different modulation indices and phases compared with the band center. It was found that bias ranges $\Delta\Gamma_{dc}$ corresponding to $\Delta\lambda > 10$ nm could give erroneous results, for example, $P(\omega)/P(0) > 1$.

Observed fiber output power levels are on the order of 1 nanowatt. The Varian VPW-154/2 static crossed-field photomultiplier tube* is particularly suitable for our broadband low light level application. Due to the crossed electric and magnetic fields formed by applied voltages and integral magnets, detected photoelectrons travel a cycloidal path and are multiplied by six dynodes before being collected at the anode. These short tightly focused electron paths result in the high 0 to 2.5-GHz detection bandwidth necessary for our measurements. The tube has an InGaAsP photocathode sensitive to far infrared wavelengths up to 1100 nm and its six dynode stages provide 3×10^5 gain. The resultant anode sensitivities yield high signal-to-noise ratios with 10-KHz spectrum-analyzer bandwidths. Additional problems of rf interference from the high-power rf oscillator picked up on the spectrum analyzer were eliminated by carefully shielding the modulator circuitry and the photomultiplier housing.

1.2 Frequency domain measurements

Input-to-output power-transfer functions have been measured from dc to 1 GHz in a variety of germanium and boron-doped kilometer-length fibers. Wavelength-dependent measurements were made by filtering the white arc lamp light through a series of interference filters whose center wavelengths ranged from $\lambda = 650$ nm to $\lambda = 1100$ nm. To reduce modulator errors and material dispersion effects,[12] the filter bandwidths were less than: 1.5 nm for 650 nm $< \lambda <$ 908 nm, 2.4 nm for 920 nm $< \lambda <$ 980 nm, and 10 nm for 1040 nm $< \lambda <$ 1100 nm.

The least-dispersive test fiber was a graded borosilicate fiber with $\alpha \sim 1.8$, which had a 1-dB bandwidth of 1 GHz after 1.07 km of propagation at $\lambda = 908$ nm. Figure 2a illustrates its sideband output power normalized to dc, $P(f)/P(0)$, plotted versus modulating frequency for six wavelengths in the range 650 nm $< \lambda <$ 1100 nm. The frequency bandwidth increases with increasing wavelength. This trend is clearer in Fig. 3a, which shows relative sideband power plotted versus 14 wavelengths for a fixed modulation frequency, $f = 990$ MHz. The 25-percent increase in bandwidth in the range 650 nm $< \lambda <$ 1100 nm is partially due to material dispersion effects, which decrease as the wavelength increases. Material dispersion should cause a 1-dB amplitude roll-off after 1 GHz for 1.5-nm source spectral

* Varian/LSE Division, Palo Alto, California.

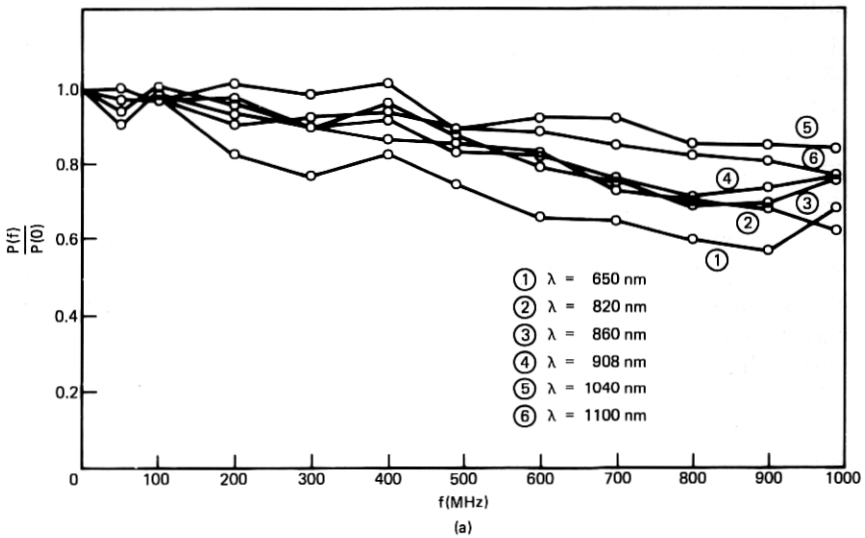

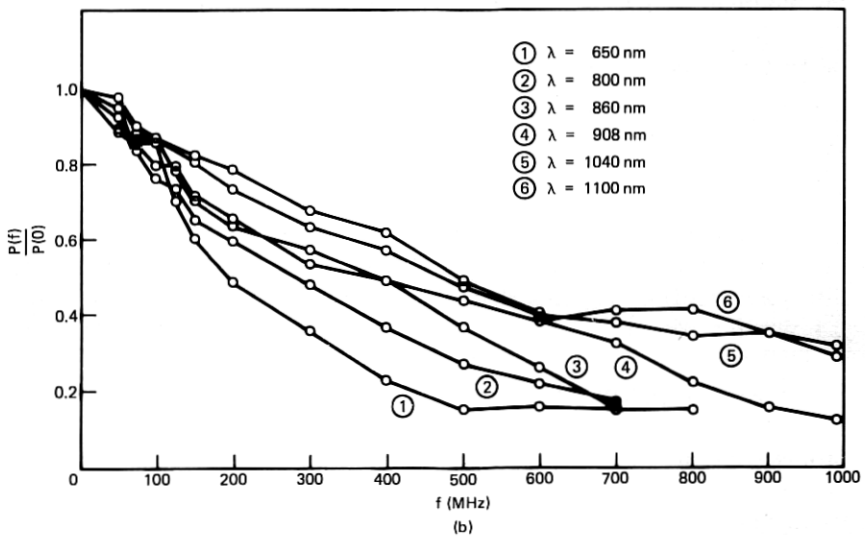

Fig. 2—Power transfer function amplitude vs. modulation frequency with optical wavelength as parameter. (a) Boron-doped graded-core fiber. (b) Germanium-doped graded-core fiber.

bandwidths centered about wavelengths between 650 nm $< \lambda <$ 750 nm. If the sideband amplitudes were increased by 1 dB between 650 nm $< \lambda <$ 750 nm to compensate for material dispersion, then the resultant data points in Fig. 3a would be independent of wavelength for 650 nm $< \lambda <$ 1100 nm.

Figure 2b illustrates power transfer functions for a graded germanium-doped fiber with $\alpha \sim 1.9$, which does not have a near-optimal profile for minimum modal dispersion. As a result, it has a relatively narrow 1-dB bandwidth of 150 MHz after 0.9 km of propagation at a wavelength of 908 nm. Material dispersion effects should be negligibly small here because amplitude roll-offs are much faster than in Figs. 2a and 3a. Hence, profile dispersion is responsible for the wavelength dependence of the bandwidth broadening in this fiber. The wavelength-dependent broadening is much greater for this germanium-doped fiber than for the previously described boron-doped fiber. Figure 3b shows relative sideband power plotted versus 14 wavelengths for a fixed modulation frequency, $f = 100$ kHz. The bandwidth more than doubles for 650 nm $< \lambda <$ 1100 nm. Comparison of curves a and b in Fig. 3 suggests that wavelength variation of profile dispersion is significantly greater in germanium-doped fibers than in boron-doped fibers. This observation is qualitatively consistent with recent refractive index profile measurements by interference microscopy on thin polished fiber samples.[13]

1.3 Equivalence of impulse and frequency domain measurements

We can prove (1) and (2) neglecting material dispersion for the simple case of a multimode fiber transmitting an incoherent optical beam without mode mixing as follows. Although a general proof is given by Personick,[2] the following proof is more relevant to our

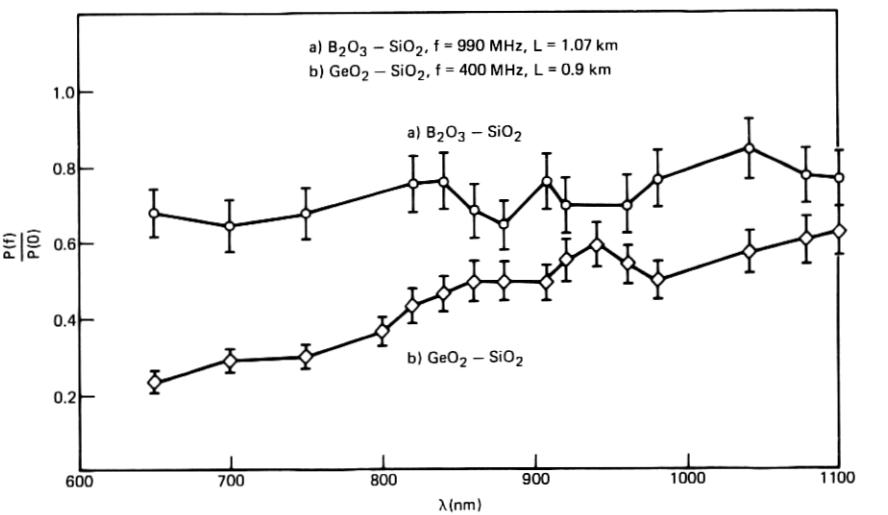

Fig. 3—Power transfer function amplitude vs. optical wavelength with modulation frequency as parameter. (a) Boron-doped graded-core fiber. (b) Germanium-doped graded-core fiber.

measurement technique. Assume an input amplitude pulse defined by

$$e_{\text{in}}(t) = v(t)e^{i\omega_o t}, \tag{4}$$

and corresponding power pulse defined by

$$p_{\text{in}}(t) = |v(t)|^2, \tag{5}$$

where $\omega_o(t)$ is the fluctuating frequency of the incoherent optical carrier and $v(t)$ is the envelope of a short pulse with peak at $t = 0$. If the input pulse excites N modes of the fiber such that the fractional power in the ν-th mode is $|c_\nu|^2$, then the output is

$$e_{\text{out}}(t) = \sum_{\nu=1}^{N} c_\nu v(t - \tau_\nu)e^{i\omega_o(t-\tau_\nu)} \tag{6}$$

$$p_{\text{out}}(t) = \sum_{\nu=1}^{N}\sum_{\mu=1}^{N} c_\nu c_\mu^* v(t - \tau_\nu)v^*(t - \tau_\mu)e^{i\omega_o(\tau_\mu-\tau_\nu)}, \tag{7}$$

where τ_ν is the delay for ν-th mode and

$$\sum_{\nu=1}^{N} |c_\nu|^2 = 1. \tag{8}$$

Now $p_{\text{out}}(t)$ is measured by a detector with response time T_1 that is usually comparable with the output pulse width, say $T_2 > 10^{-10}$ s. The incoherent optical carrier at $\lambda \approx 10^3$ nm with $\Delta\lambda \sim 1$ nm has a frequency bandwidth $\Delta\omega_o = 2\pi c\Delta\lambda/\lambda^2 \approx 2\pi \times 3 \times 10^{11}$ Hz that can be regarded as arising from a random frequency modulation of the carrier with modulation frequency ω_m and deviation frequency ω_d both roughly equal to $\Delta\omega_o$. But, $d\omega_o/dt = \omega_m\omega_d \approx (\Delta\omega_o)^2$ for an FM signal. Then, the phase factor $\omega_o(\tau_\mu - \tau_\nu)$ will fluctuate through a phase range $\Delta\phi$ of at least

$$\Delta\phi = (d\omega_o/dt)(\tau_\mu - \tau_\nu)T_1 \approx (\Delta\omega_o)^2(\tau_\mu - \tau_\nu)T_1 \approx (\Delta\omega_o)^2 T_1 T_2/N \text{ radians} \tag{9}$$

during the characteristic measuring time T_1 for an N-mode fiber. If $(\tau_\mu - \tau_\nu)$ is the minimum delay difference between adjacent, equispaced modes, then T need not be smaller than $N(\tau_\mu - \tau_\nu)$, a lower bound on the output pulse width as assumed in (9). Thus, we find $\Delta\phi > 100\pi$ for $N = 100$ and $T_1 = T_2 > 10^{-10}$ s, so that all terms in (7) for $\nu \neq \mu$ vanish on averaging over T. In the present experiment, $T = 10^{-4}$ s as determined by the spectrum analyzer bandwidth so that $\Delta\phi \gg 100\pi$. Spatial incoherence of the input beam further reduces[2] the crossterms in (7).

The observed power is then

$$p_{\text{out}}(t) = \sum_{\nu=1}^{N} |c_\nu|^2 |v(t - \tau_\nu)|^2, \tag{10}$$

and if we let $|v(t)|^2$ be the unit impulse $u_0(t)$, we have the impulse response

$$g(t) = \sum_{\nu=1}^{N} |c_\nu|^2 u_0(t - \tau_\nu). \tag{11}$$

The Fourier transform of the impulse response yields

$$\begin{aligned} G(\omega) &= \int_{-\infty}^{\infty} g(t) e^{-i\omega t} dt \\ &= \sum_{\nu=1}^{N} |c_\nu|^2 e^{-i\omega\tau_\nu}, \end{aligned} \tag{12}$$

where ω is the frequency of the envelope of the modulated carrier and $G(\omega)$ is the complex power transfer function.

Next, consider a sinusoidally intensity-modulated incoherent carrier incident on the fiber. This is the experimental method used here. We wish to show it to be equivalent to the impulse response method. For sufficiently small modulation index m, the electrooptically modulated input to the fiber is

$$e_{\text{in}}(t) = (1 + m \cos \omega t)^{\frac{1}{2}} e^{i\omega_0 t} \tag{13}$$

$$p_{\text{in}}(t) = (1 + m \cos \omega t). \tag{14}$$

Since we employ a spectrum analyzer in the measurements, we are concerned only with the term at the fundamental frequency ω in (14). As before, the input excites N modes of the fiber and the output is

$$e_{\text{out}}(t) = \sum_{\nu=1}^{N} c_\nu e^{i\omega_0 (t-\tau_\nu)} [1 + m \cos \omega(t - \tau_\nu)]^{\frac{1}{2}} \tag{15}$$

$$\begin{aligned} p_{\text{out}}(t) = \sum_{\mu=1}^{N} \sum_{\nu=1}^{N} & c_\nu c_\mu^* e^{i\omega_0 (\tau_\mu - \tau_\nu)} \\ & \times [1 + m \cos \omega(t - \tau_\nu)]^{\frac{1}{2}} [1 + m \cos \omega(t - \tau_\mu)]^{\frac{1}{2}}. \end{aligned} \tag{16}$$

But we can use our earlier argument for the random carrier to eliminate all terms for $\nu \neq \mu$ in (16). If we retain only the term at the fundamental frequency, we obtain the observed power

$$p_{\text{out}}(t) = m \sum_{\nu=1}^{N} |c_\nu|^2 \cos \omega(t - \tau_\nu) = \text{Re} \left\{ m \sum_{\nu=1}^{N} |c_\nu|^2 e^{-i\omega\tau_\nu} e^{i\omega t} \right\}. \tag{17}$$

Then, with $\tau_\nu = 0$ for $p_{\text{in}}(t)$,

$$\frac{P_{\text{out}}(\omega)}{P_{\text{in}}(\omega)} = G(\omega) = \sum_{\nu=1}^{N} |c_\nu|^2 e^{-i\omega\tau_\nu} \tag{18}$$

as in (12), which completes the proof of equivalence for no mode mixing. With mode mixing, τ_ν becomes a continuum,[2] and we must simply replace the sum in (12) and (18) by an integral over the range of τ, i.e.,

$$G(\omega) = e^{-i\omega\tau_0} \int_{-T_a}^{T_b} |c(\tau')|^2 e^{-i\omega\tau'} d\tau' = |G(\omega)| e^{-i\omega\tau_0} e^{i\theta}, \tag{19}$$

where

$$\tau = \tau_0 + \tau', \tag{20}$$

and τ_0 is the (large) average delay, τ' is the deviation from τ_0, and $-T_a < \tau' < T_b$ is the range of allowed modal delay. In a similar way for (18), we can let

$$\tau_\nu = \tau_0 + \tau'_\nu. \tag{21}$$

At present our measurements yield only $|G(\omega)|$. The phase angle $\theta(\omega)$ is required to obtain the impulse response $g(t)$ from

$$g(t) = \frac{1}{2\pi} \int_{-\infty}^{\infty} G(\omega) e^{i\omega t} d\omega. \tag{22}$$

Direct measurement of $\theta(\omega)$ is difficult because a 1-km long fiber contains many modulation wavelengths. However, if we assume that the fiber behaves like a minimum phase network, i.e., $G(j\omega)$ has no zeros in the right half of the complex plane, then we can calculate $\theta(\omega)$ from $|G(\omega)|$. The average delay factor $e^{-i\omega\tau_0}$ is not a minimum phase function.[14] However, $G(\omega)e^{i\omega\tau_0}$ in (18) and (19) appears to exhibit approximate minimum phase behavior in some, but not all cases. In the next section we illustrate the approximate minimum phase behavior as obtained from a comparison of the $g(t)$ calculated from $|G(\omega)|$ with the measured $g(t)$ for a particular fiber. A later publication will treat the minimum phase approximation in more detail.

On the other hand, the measured $g(t)$ is real so that $G(\omega)$ may be obtained directly from pulse measurements using (12) without any assumptions as we also show below.

1.4 Correlation with time domain measurements

The impulse response $g(t)$ was measured by injecting narrow impulses ($2\sigma = 0.4$ ns) from a GaAs laser and observing the broadened output. Time domain measurements were fast-Fourier-transformed to produce the solid curves shown in Fig. 4a and b for the boron and germanium-doped fibers described in Figs. 2 and 3. Time domain data

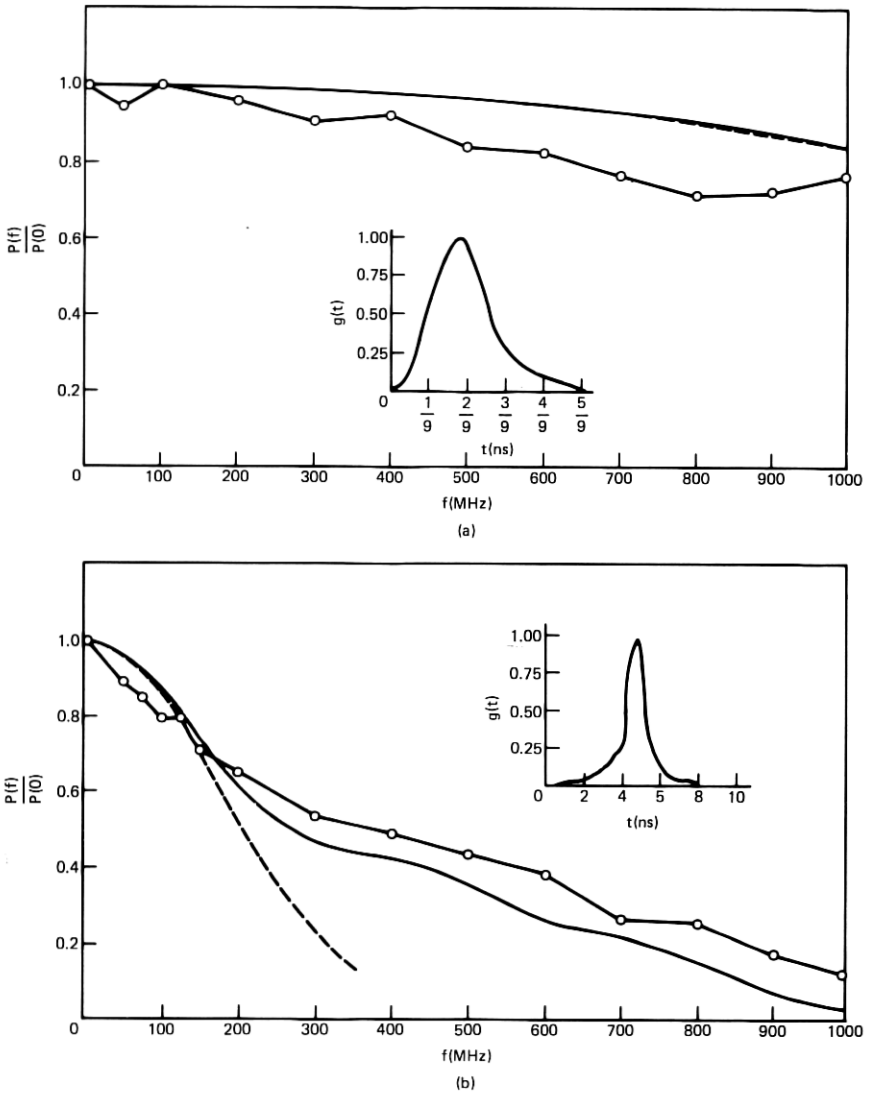

Fig. 4—Frequency domain measurements (0 data points) are compared with fast-Fourier transformed impulse response measurements $[g(t)$ vs. $t]$ at $\lambda = 908$ nm, $\Delta\lambda \approx 1.4$ nm. The dashed curves are gaussian fits to the solid curves (computed transforms). (a) Boron-doped graded-core fiber, $2\sigma = 0.19$ ns/1.07 km. (b) Germanium-doped graded-core fiber, $2\sigma = 1.8$ ns/0.9 km.

for the low dispersion borosilicate fiber (inset Fig. 4) was deduced from shuttle pulse measurements after nine trips through the fiber. Fourier-transformed time domain results are compared in Fig. 4 with directly measured frequency domain data points measured in incoherent light

at the same wavelength, $\lambda = 908$ nm. The qualitative agreement is quite good and the quantitative agreement is generally within 20 percent. Dashed curves in Fig. 4a and b show gaussian approximations to the computed solid curves given by

$$|G(\omega)| \approx e^{[-(\omega\sigma)^2/2]}, \tag{23}$$

where 2σ is the full rms pulse width of the measured impulse responses, $g(t)$, illustrated in the insets of Fig. 4a and b ($2\sigma \approx 0.19$ ns/1.07 km for the boron-doped fiber a; $2\sigma \approx 1.8$ ns/0.9 km for the germanium-doped fiber b. Thus, the gaussian fit to $|G(\omega)|$ can give an estimate of the pulse width 2σ without knowledge of $\theta(\omega)$.

In both cases a and b, the gaussian approximations to $|G|$ are accurate down to the 0.75-amplitude point in the frequency domain. The approximation does not fit the germanium fiber b data, when $|G(\omega)| < 0.75$, because its impulse response is asymmetric with a long leading edge.

The usefulness of the minimum phase approximation, for inverting frequency domain amplitude spectra back into the time domain, was tested on data in Figs. 2b and 4b for a germanium-doped fiber. A Hilbert transform was used to compute the minimum phase function, $\theta(f)$, from the $\ln |G(\omega)| = -\eta(\omega)$,[14]

$$\theta(f) = -\frac{f}{\pi}\int_{-\infty}^{\infty} \frac{\eta(f_0)}{f_0^2 - f^2}\, df_0. \tag{24}$$

Hilbert transforms are particularly easy to evaluate when the given function, $\eta(f)$, is a piecewise-linear function consisting of a series of M straight-line segments. In that case its second derivative consists of a sum of impulses and the integral formulation of (24) can be replaced by a summation.[14]

$$\theta(f_m) = -\frac{1}{\pi}\sum_{K=1}^{M} B(K)[(f_m - f_K)\ln|f_m - f_K| + (f_m + f_K)\ln|f_m + f_K|], \tag{25}$$

where

$$B(K) = A(K+1) - A(K)$$

$$A(K) = \frac{\eta(f_{K+1}) - \eta(f_K)}{f_{K+1} - f_K}.$$

Figure 5a uses the data in Fig. 4b to compare: curve 1, the measured impulse response shown in Fig. 4b, with detector distortion deconvolved ($2\sigma = 1.81$ ns), and curve 2, the time pulse obtained by taking the Fourier transform of 1 and using its amplitude spectrum and assumed minimum phase to compute the impulse response ($2\sigma = 1.77$ ns). Curve 3 shows the time pulse calculated from frequency measurements in Fig. 4b and the corresponding piecewise linear minimum phase function ($2\sigma = 1.89$ ns). The rms pulsewidths and qualitative

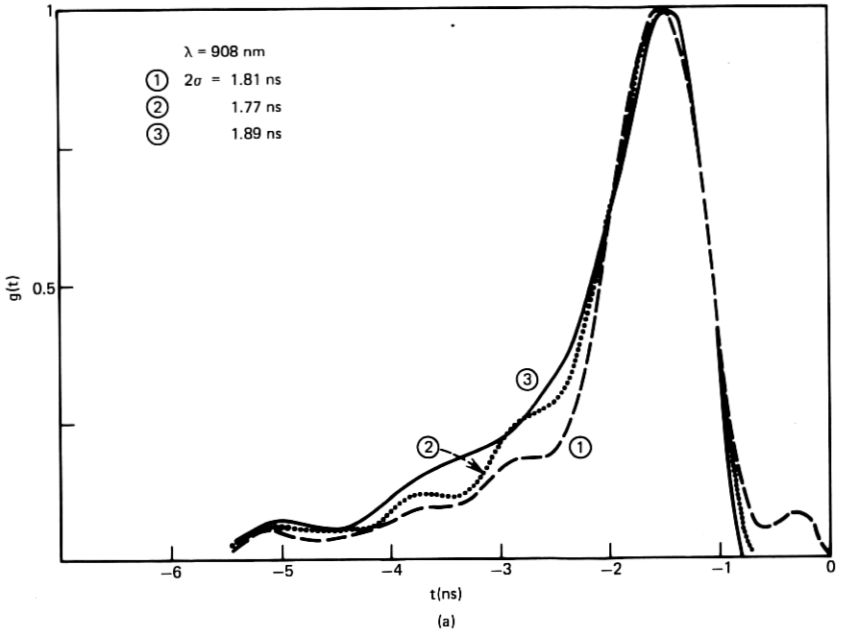

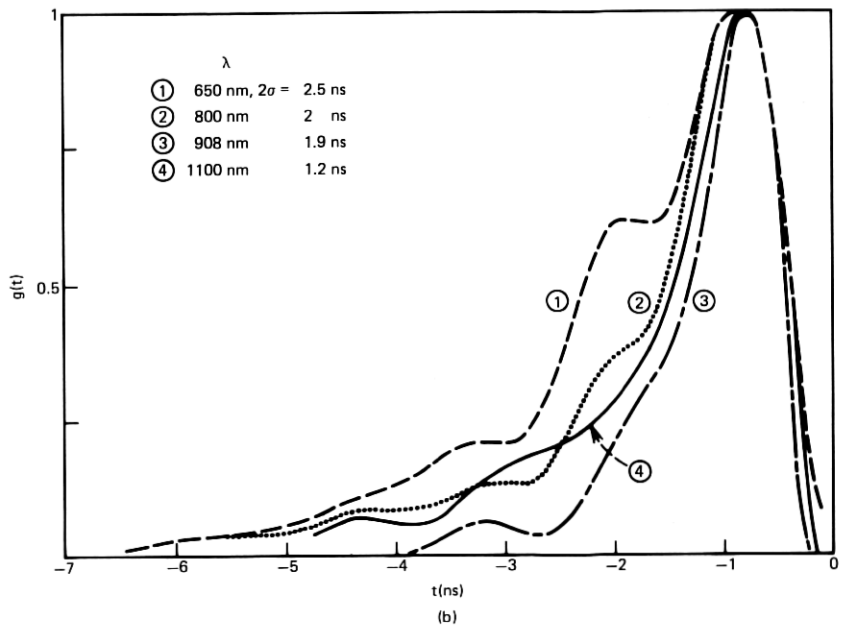

Fig. 5—Time domain impulse responses computed from amplitude spectra in the frequency domain. (a) A measured impulse response at $\lambda = 908$ nm (1) is compared with (2) its minimum phase response, and (3) the response using frequency domain measurements in Fig. 4b and minimum phase function assumption. (b) Wavelength-dependent time pulses computed from frequency domain measurements in Fig. 2b.

structure of the three pulses in Fig. 5a agree very well, which implies that the minimum phase function can be used to construct a good facsimile of the actual impulse response.

Minimum phase functions were also calculated for data in Fig. 2b and used to construct the wavelength-dependent impulse response shapes in Fig. 5b. The results show that the impulse response becomes wider and more asymmetric when the signal wavelength is reduced from $\lambda = 1100$ nm ($2\sigma = 1.2$ ns) to $\lambda = 650$ nm ($2\sigma = 2.5$ ns).

II. CONCLUSIONS

The baseband frequency response of kilometer-long graded index fibers have been directly measured over a 0 to 1 GHz frequency range for wavelengths extending from the visible ($\lambda = 650$ nm) into the infrared ($\lambda = 1100$ nm). The accuracy of individual sideband measurements is approximately 10 percent, which is equivalent to a time resolution of $2\sigma = 0.15$ ns (assuming a gaussian frequency roll-off function $e^{[-(\omega\sigma)^2/2]}$ at $f = 1$ GHz). By contrast, full rms pulse width measurements in the time domain would require a precision of $\sqrt{(0.15)^2 + (2\sigma_i)^2} - 2\sigma_i \approx 0.02$ ns to achieve the same resolution from measurements deconvolved from detector-limited input pulse widths with $2\sigma_i \approx 0.4$ ns.

The major advantage of the spectral technique described here is its convenience for making wavelength-dependent measurements with a tunable source of incoherent light.

The least-dispersive-measured fiber, with NA ≈ 0.14 and graded borosilicate core, had an 80-percent transmission bandwidth, F (1 dB) ≈ 1 GHz/1.07 km ($\lambda = 908$ nm, $\Delta\lambda \approx 1.4$ nm), which is approximately equivalent to a full rms pulse width $2\sigma = 0.2$ ns/km. The fiber bandwidth broadened by about 25 percent over the wavelength range 650 nm $< \lambda <$ 1100 nm. However, a significant fraction of that increase between 650 nm $< \lambda <$ 820 nm can be attributed to material dispersion effects, which are insignificant for $\lambda >$ 820 nm. For comparison, a germanium-doped fiber with NA ≈ 0.2 had a bandwidth F (1 dB) ≈ 0.15 GHz/0.9 km ($\lambda = 908$ nm, $\Delta\lambda \approx 1.4$ nm), which is approximately equivalent to a full rms pulse width $2\sigma = 2$ ns/km. Fiber bandwidth broadened by about 250 percent due to profile dispersion over the wavelength range 650 nm $< \lambda <$ 1100 nm. Less than 5 percent of this wavelength dependence can be attributed to material dispersion caused by the 1.5 nm spectral bandwidths of the filtered incoherent signal light. The fact that germanium-doped fibers exhibit much more profile dispersion than boron-doped fibers is in good agreement with interference microscopy measurements on thin fiber samples.[13]

The rms pulse width 2σ can be estimated from the transfer function amplitude $|G(\omega)|$ by assuming a gaussian distribution (23). In some cases, the shape of the pulse can be obtained by assuming a minimum phase transfer function. This latter method was used to compute wavelength-dependent time pulses from frequency response measurements in the germanium-doped fiber described. Profile dispersion made impulse response shapes wider and more asymmetric when the signal wavelength was reduced from $\lambda = 1100$ nm ($2\sigma = 1.2$ ns) to $\lambda = 650$ nm ($2\sigma = 2.5$ ns).

III. ACKNOWLEDGMENTS

We are grateful to F. S. Chen for providing the $LiTaO_3$ modulator and to D. Enck and R. Klein (Varian/LSE Division) for their help with the crossed-field photomultiplier detector. We also thank W. Mammel for her help in computing the FFT and minimum phase functions, W. G. French, J. B. MacChesney, P. B. O'Connor, and G. W. Tasker for providing the fibers, and S. D. Personick for useful discussions of the theory.

REFERENCES

1. L. G. Cohen, "Shuttle Pulse Measurements of Pulse Spreading in an Optical Fiber," Appl. Opt., *14* (June 1975), pp. 1351–1356.
2. S. D. Personick, "Baseband Linearity and Equalization in Fiber Optic Digital Communication Systems," B.S.T.J., *52* (September 1973), pp. 1175–1194.
3. D. Gloge and E. A. J. Marcatili, "Multimode Theory of Graded-Core Fibers," B.S.T.J., *52* (November 1973), pp. 1563–1577.
4. R. Olshansky and D. B. Keck, "Pulse Broadening in Graded-Index Optical Fibers," Appl. Opt., *15* (February 1976), p. 491.
5. D. Gloge, I. P. Kaminow, and H. M. Presby, "Profile Dispersion in Multimode Fibers—Measurement and Analysis," Electron. Lett., *11* (September 1975), pp. 469-470.
6. J. W. Fleming, "Measurements of Dispersion in GeO_2-B_2O_3-SiO_2 Glasses," Fall Meeting of the Amer. Ceram. Soc., Pocono Manor, October 1975.
7. L. G. Cohen, "Pulse Transmission Measurements for Determining Near Optimal Profile Gradings in Multimode Borosilicate Optical Fibers," Appl. Opt., *15* (July 1976), pp. 1808–1814.
8. D. Gloge, E. L. Chinnock, and D. H. Ring, "Direct Measurement of the (Baseband) Frequency Response of Multimode Fibers," Appl. Opt., *11* (July 1972), pp. 1534–1538.
9. R. Auffret, C. Boisrobert, and A. Cozannet, "Wobulation Technique Applied to Optical Fibre Transfer Function Measurement," First European Conference on Optical Fibre Communication, IEE, London, England (September 16–18, 1975), pp. 60–63.
10. S. D. Personick, W. M. Hubbard, and W. S. Holden, "Measurements of the Baseband Frequency Response of a 1-Km Fiber," Appl. Opt., *13* (February 1974), pp. 266–268.
11. F. S. Chen, "Modulators for Optical Communications," Proc. IEEE, *58* (October 1970), pp. 1440–1457.
12. D. Gloge and E. L. Chinnock, "Fiber-Dispersion Measurements Using a Mode-Locked Krypton Laser," IEEE J. Quantum Electron., *QE-8* (November 1972), pp. 852–854.
13. H. M. Presby and I. P. Kaminow, "Refractive Index and Profile Dispersion Measurements in Binary Silica Optical Fibers," Appl. Opt., February 1977.
14. E. A. Guillemin, *Theory of Linear Physical Systems*, New York: John Wiley (1963), pp. 252, 275, and 536.